Elsevier Editorial System(tm) for Separation and Purification Technology

Manuscript Draft

Manuscript Number:

Title: On improving the CO2 recovery efficiency of a conventional TSA process in a sound assisted fluidized bed by separating heating and purging

Article Type: Full Length Article

Keywords: CO2 capture; Sound-assisted fluidization; Activated carbon; TSA; Adsorption; Desorption.

Corresponding Author: Dr. Paola Ammendola, Ph.D.

Corresponding Author's Institution: CNR

First Author: Federica Raganati, PhD

Order of Authors: Federica Raganati, PhD; Paola Ammendola, Ph.D.; Riccardo Chirone, PhD

Dear Editor,

enclosed please find the manuscript “On improving the CO_2 recovery efficiency of a conventional TSA process in a sound assisted fluidized bed by separating heating and purging” to be submitted for publication as research paper in Separation an Purification Technology journal. The submission is original, not under consideration for publication elsewhere, and all authors are aware of the submission and agree to its publication.

Sincerely yours

Paola Ammendola

Graphical Abstract

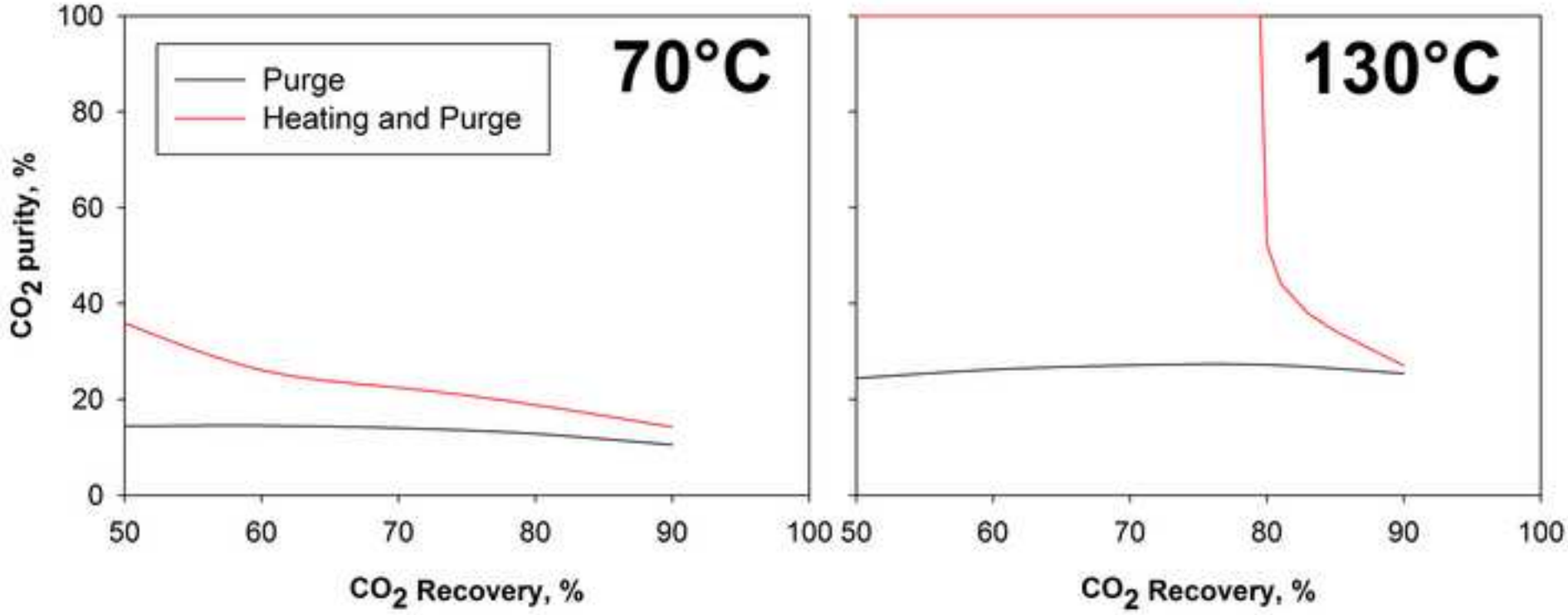

Highlights

1. Separate heating and purge regeneration strategy has been tested for CO_2 recovery.
2. Heating is very efficient for desorbing carbon dioxide.
3. 80% CO_2 recovery can be obtained at 130°C by sole thermal effect.
4. 100% vol. CO_2 purity with recovery >50% can be obtained for temperature ≥100°C.
5. 100% vol. CO_2 purity can be obtained even in a cyclic process.

On improving the CO_2 recovery efficiency of a conventional TSA process in a sound assisted fluidized bed by separating heating and purging

Federica Raganati, Paola Ammendola*, Riccardo Chirone

Istituto di Ricerche sulla Combustione, CNR, P.le V. Tecchio, 80-80125 Napoli, Italy

*Corresponding author
Tel.:+39 0817682237; fax:+39 0815936936.
E-mail address: paola.ammendola@irc.cnr.it

Abstract

Carbon capture from point source emissions has been recognized as one of several strategies necessary for mitigating release of greenhouse gases (GHGs) into the atmosphere. Though several CO_2 capture technologies have been proposed, temperature swing adsorption (TSA), consisting in adsorbing the CO_2 and, then, recovering it by a temperature increase and gas purge, is currently believed to be one of the most promising for post-combustion applications. With reference to the sorbent, great attention is focused on fine powders. Indeed, sorbent in the form of fine powders can be the substrate to realize new highly specific materials whose properties can be tuned at a molecular level and, besides that, most of the commercial adsorbent materials are generally available in the form of fine powders. Previous works successfully verified the feasibility of carrying out TSA adsorption/desorption cycles in a sound assisted fluidized bed, thus enhancing the performances of the entire cyclic process. The focus of the present work is to overcome the main drawback of a conventional TSA, namely the dilution of CO_2 in the purging gas. To this aim, a separate heating and purge regeneration strategy, consisting in desorbing part of the CO_2 by the sole thermal effect, has been tested on a commercial activated carbon, thus eliminating the unavoidable dilution effect caused by purge, and the remainder reducing the CO_2 partial pressure. Heating is very efficient for desorbing CO_2. Indeed, 80% of the captured CO_2 can be recovered at a bland temperature of 130°C.

Keywords: CO_2 capture; Sound-assisted fluidization; Activated carbon; TSA; Adsorption; Desorption.

1 Introduction

Increasing awareness of the influence of greenhouse gases on global climate change has led to recent efforts to develop strategies for the reduction of CO_2 emissions [1]. One of the strategy that is receiving the greatest attention involves the capture of CO_2 from large point sources, such as fossil fuel-fired power plants, and long-term storage underground or in the ocean [2]. CO_2 capture can be achieved by either post- or pre-combustion capture at ambient or high pressure, respectively [3]. Aqueous solutions of amines have long been used by industry as absorbents for acid gas (CO_2, H_2S) removal, but have a large number of shortcomings when applied to a flue gas, i.e. characterized by low CO_2 partial pressure [4]. As an alternative, adsorption is one of the most promising technologies for post combustion capturing CO_2 from flue gases, potentially avoiding the weaknesses of aqueous amine systems and offering potential energy savings with lower capital and operating costs [5-8].

However three major aspects will determine the success of adsorption as CO_2 capture technique: the choice of adsorbent materials, regeneration strategy and reactor configuration [9,10].

With reference to the adsorbent materials, much of the worldwide research activity is now focused on development of novel sorbents whose physico-chemical properties can be tuned and controlled at the molecular level [5, 11-14]. To this aim, fine particles are particularly versatile since they can be simply adjusted according to the application requirements: due to their special size and shape, ultra-fine particles are particularly suitable to be easily tailored and/or functionalized on the surface with different ligands to induce significant changes in their physical and chemical properties [5, 11-14]. Besides, also common and commercially available adsorbent materials (such as activated carbons and zeolites) are generally in the form of fine powders.

Regarding the choice of the regeneration strategy, temperature swing adsorption (TSA) is one of most promising alternatives among all the other technological options [7,8,15], i.e. pressure swing adsorption (PSA) [8], vacuum swing adsorption (VSA) [16] and electric swing adsorption (ESA) [17], when applied under post-combustion conditions [10]. In a conventional TSA regeneration

process the sorbent temperature is increased by purging the bed with a preheated purging gas (e.g. steam or N_2). Due to the low heat capacity of gases, a large volume of gas is required to heat the bed, thus leading to the desorption of the CO_2 diluted in the heating gas [15,18]. As a possible way to avoid this problem, the heat for regeneration of the solid can be provided by indirect heating (e.g. via heat exchanger tubes), instead of directly contacting the solid with hot gas that flows through the bed, thus remarkably reducing the volume of purge gas and limiting the dilution effect [15,18]. In this way, no carrier gas is used to induce the desorption of CO_2 and the desorbed gas can be recovered by thermal expansion, thus obtaining a pure CO_2 stream as desorption gas and in turn overcoming the dilution problem [15].

Finally, with reference to the reactor configuration, common adsorption operations are generally performed in fixed-bed reactors. However, this configuration does not appear to be the best choice neither to fully exploit the potential of fine sorbents nor to properly perform a regeneration strategy based on a thermic process [16,19,20]. Indeed, for fine materials to be used in fixed bed operations, a previous pelletization step is needed in order to overcome the prohibitively high pressure drops related to fine particle beds. However, after the shaping processes (usually performed using a press or an extrusion method), the specific surface area could dramatically decrease, and some pores could be blocked, thus leading to a decline in adsorption capacity [19]. In addition, temperature swing in fixed bed reactors, serving as both the adsorber and the regenerator, is naturally inefficient because poor local heat dissipation for the exothermic adsorption reactions and poor heat transfer to the solid sorbents for the endothermic regeneration reactions will produce local “hot” and “cold” spots, respectively, preventing efficient conversions [16,19,20]. In this framework, a fluidized bed could be a possible alternative. Firstly, it is capable of directly using and process large quantities of free-flowing fine powders and, moreover, fluidized beds are characterized by high heat transfer coefficients between particles and gas, thus providing an easier temperature control during both adsorption and regeneration step [9,10].

However, fine powders, belonging to the C group of Geldart's classification [21], cannot be fluidized under ordinary conditions, because of the characteristic cohesive forces (such as van der Waals, electrostatic and moisture-induced surface tension forces) existing between particles and increasing as the particle size decreases [21]. Therefore, a good fluidization regime can be achieved using different externally assisted fluidization techniques, all of them based on the application of additional forces generated, for example, by acoustic [22-25], electric [26], magnetic fields [27] or mechanical vibrations [28] to enhance the dynamics of the powder in the fluidized bed. Among all these techniques sound-assisted fluidization is reported to be one of the most promising alternative, since the application of acoustic fields does not require any material modification, it is rather cheap and can be easily implemented and scaled-up from using common acoustic devices [22-25].

The efficiency of the sound application was demonstrated for both CO_2 adsorption [29-33] and desorption by TSA [9,10,30]. In particular, Raganati et al. (2014) [29,31] verified the capability of sound-assisted fluidization to positively affect the CO_2 adsorption performances of fine sorbents with respect to common technologies, such as fixed bed, due to the efficient gas-solid contact (namely maximizing the exploitation of the solid sorbent surface exposed to the fluid phase). Indeed, the application of the acoustic fields makes it possible to obtain remarkably higher breakthrough time, adsorption capacity, fraction of bed utilized until breakthrough and adsorption rate [29,31]. With reference to the desorption step, the application of the sound also results in a remarkable enhancement of the desorption efficiency [10]. In particular, the desorption rate is increased with respect to the ordinary tests (i.e. the time needed to get the same CO_2 recovery decreases with the application of the sound) and also recovered CO_2 stream is much more concentrated, up to 32% more concentrated than under ordinary fluidization conditions [9].

As shown by Raganati et al. [10] CO_2 recovery and purity have opposing trends, therefore, it is necessary to find the most convenient compromise between the two of them. In light of these considerations, a regeneration method based on TSA has been tested in the present work in order to improve the performances in the desorption step, namely find a possible way to enrich the

recovered CO_2 stream with respect to the standard regeneration strategy (desorption by purge at a fixed temperature) studied in a previous work [9]. The idea lying at the basis of this regeneration strategy is to discriminate the contribution to the CO_2 recovery given by heating from that given by purge, whereas in the standard regeneration strategy the thermal effect cannot be distinguished by that given by purge since they happen contextually. To this aim, CO_2 is desorbed in two separate phases: a heating step followed by a purge step. In particular, during the external heating the CO_2 can be desorbed without the use of any carrier gas and the desorbed gas could be recovered by thermal expansion, thus completely eliminating the dilution problem (pure CO_2 stream as desorption gas). Both adsorption and desorption tests have been carried out in a lab-scale sound assisted fluidized bed, using a commercial activated carbon as adsorbent material. Different desorption temperatures (40, 70, 100, 130, 150 °C) have been tested. In particular, desorption efficiency was assessed in terms of CO_2 recovery level and purity. Finally, this regeneration strategy was also tested in a cyclic adsorption/desorption operation.

2 Material and methods

2.1 Experimental apparatus

The laboratory scale sound-assisted fluidized bed (Fig. 1) is made of a Pyrex column (40 mm ID and 1500 mm high) equipped with a porous gas distributor plate located at 300 mm from the bottom of the column. The section of the column below the gas distributor acts as wind-box: it is filled with Pyrex rings, thus maximizing the uniformity of the gas flow entering the fluidized bed. This solution provides a good dispersion of the fluidizing gas, thus limiting fluidization troubles due to the formation of preferential channels, namely the feed of the fluidizing gas through a limited number of points. In addition, during the regeneration phase this section of the reactor also acts as a pre-heating chamber for the fluidizing gas.

The acoustic field is introduced inside the column through an ad-hoc designed sound wave guide [24]. The sound-generation system consists of a digital signal generator, a power audio amplifier rated up to 40 W and a 8 W woofer loudspeaker. More detailed information about the sound generation and insulation system can be found elsewhere [24].

A temperature probe is located at 400 mm from the top of the column. In particular, the temperature inside the reactor is monitored at the center of the bed (60 mm from the gas distributor) by means of a type K thermocouple (Chromel-Alumel) with a diameter of 1 mm. This thermocouple is connected to a temperature controller in order to monitor it during the experimental tests and keep it at the desired value. A heating jacket (Tyco Thermal Controls GmbH) is wrapped around its external surface to heat the column to the desired desorption temperature. In particular, it has been ad-hoc designed: it is 500 mm high with an isothermal height of 350 mm and it is also provided with a window, which allows the fluidization quality to be visually assessed also during the desorption step.

Gas feed is made using separate N_2 (99.995%) and CO_2 (99.995%) cylinders. The flowrates have been set and controlled by two mass flow controllers (Brooks 8550S). The exit gas flow rate during the heating step is measured using a volumetric flowmeter (Brooks 4800S).

The analysis system consists of a continuous analyzer, to monitor the outlet CO_2 concentration in a transient adsorption/desorption process by means of an infrared (AO2020, URAS 14) detector. Only a fraction of the outlet gas stream is taken and sent to the analysis. In particular, the gas sampling is performed by means of a pump (SCC-S sample gas feed unit from ABB), which can sucks at the desired flow rate from a sampling probe located at 400 mm from the top of the column. Since the analysis system is made of very sensitive devices, a ceramic filter, able to capture all the elutriated fine particles, has been placed downstream the outlet of the column and before the inlet to the pump, thus preventing any damage to both the pump and the analyzer. The remaining part of the outlet gas flow rate is sent to the stack.

2.2 Adsorbent material

An activated carbon DARCO FGD (Norit) was used as adsorbent material. Detailed information on its chemico-physical and fluid-dynamic characterization are reported elsewhere [29]. In brief, it is a submicronic powder (0.39 μm) [29], belonging to the C group of Geldart's classification [21]. It is characterized by a large BET surface area (1060 m^2g^{-1}) and by a broad pore size distribution: both mesoporespores (2 nm < d < 50 nm) and micropores (d < 2 nm) can be observed. In particular, the microporous region is bimodal with more than a half of the micropores smaller than 0.9 nm [29].

With regard to the fluid-dynamic characterization, the application of proper acoustic fields (SPLs higher than 125 dB and frequencies in the range 50-120 Hz [29]) enhances the fluidization quality, thus resulting in a more efficient gas solid contact, which is closely related to an efficient break-up of the large aggregates yielded by cohesive forces into smaller structures easily to be fluidized [29].

2.3 Experimental procedure

TSA tests were performed at atmospheric pressure to recover the CO_2 from the spent activated carbon in the sound-assisted experimental apparatus described above, loading 110 g of activated carbon, corresponding to a bed height of about 15 cm. Before each desorption test an adsorption step is performed at ambient temperature and atmospheric pressure under sound-assisted conditions (140 dB - 80 Hz) feeding 67.8 Nl h^{-1} (i.e. a superficial gas velocity of 1.5 cm/s, which is about five times larger than the minimum fluidization velocity of the sorbent material [29]) of an inlet CO_2/N_2 mixture with a CO_2 concentration (C_0) of 10% vol.. These values of sound intensity and frequency have been proved to optimize the fluidization quality and the gas-solid contact efficiency, which, in turn, enhances the CO_2 adsorption and desorption performance of fine solid materials [29,31].

The recovery of the captured CO_2 is realized in two steps (heating and purging) so that the effect of the increasing temperature (heating) and reducing CO_2 partial pressure (purging) can be isolated, namely it has been possible to discriminate the amount of CO_2 desorbed by heating from that recovered by purge. Just after the adsorption step, the column is heated up to the desired desorption

temperature by means of the heating jacket. Desorption temperatures (40, 70, 100, 130, 150 °C) have been selected according to those typically used for activated carbons [8]. Differently from the standard regeneration strategy described in [9], during this heating step, the inlet to column is closed and the acoustic field is switched off so that the desorbed CO_2 can leave the column only due to a thermic effect (i.e. the system continuously shifts to new adsorption equilibria as the temperature increases). The exit gas flow rate (pure CO_2) is measured using a volumetric flowmeter placed at the exit of the column. When the thermodynamic equilibrium corresponding to the chosen desorption temperature was reached and the CO_2 still adsorbed to the sorbent surface could not be recovered, since the partial pressure of carbon dioxide inside the column is equal to atmospheric pressure, the exit flow rate stops and then the inlet to column is opened, the sound is switched on (140 dB–80 Hz) and N_2 is flowed at a constant flow rate of 67.8Nl h^{-1} (purge step). During this step the temperature of the column is maintained constant and the CO_2 outlet concentration is continuously monitored by analyzing a fraction of the outlet gas stream by means of the continuous analyzer.

3 Results and discussion

3.1 Desorption tests: effect of heating and purging

The desorption process efficiency has been assessed in terms of the purity of the recovered CO_2 stream and the percentage of CO_2 recovered with respect to that captured during the previous adsorption step. Details on the calculations can be found in [9]. The breakthrough curves obtained during the adsorption step, under the operating conditions described in the "Experimental procedure" section, are also reported in a previous work [29].

The CO_2 desorption profiles, in terms of total outlet flow rate, obtained at different desorption temperatures during the heating step are reported in Fig. 2a. The exit gas flow rate, which is pure CO_2, begins to increase as soon as the electric current is applied to the heating jacket. Then, it

reaches a maximum value which increases with the temperature of regeneration, whereas, the tails become longer as the regeneration temperature is lowered. Since it is impossible to get back all the carbon dioxide whatever the temperature of the regeneration because of the thermodynamic equilibrium reached, it is necessary to lower the partial pressure of CO_2, i.e. fluxing N_2 as purge gas (purge step), to recover the remainder. Fig. 2b reports the outlet CO_2 concentration profiles obtained during the purge step at the different desorption temperatures. The trend obtained is opposite to that obtained from the heating step: as the desorption temperature is increased the desorption peak becomes lower since the amount of CO_2 still adsorbed after the heating step becomes lower with increasing desorption temperatures.

The carbon dioxide recovered during both heating and purge steps has been calculated by integration of the desorption profiles. Values of recovery are reported in Table 1 and plotted in Fig. 2c. A good closure of the mass balance between the heating and purge steps has been obtained. With reference to the heating step, it is clear that increasing the desorption temperature the amount of CO_2 desorbed is increased, in agreement with the desorption peaks becoming higher with increasing desorption temperatures (Fig. 2a). This behaviour is due to the fact that at higher temperatures the thermodynamic equilibrium shifts towards conditions more and more unfavorable for adsorption, so more CO_2 is desorbed and less is still adsorbed within the activated carbon pores. Clearly, the recovery monotonically increases with the temperature, passing from a value of about 18% at 40°C up to a value of about 82% at 150°C, even though the maximum enhancement can be observed up to 130°C since already at 130°C 80% of the adsorbed CO_2 can be recovered. Therefore, heating is very efficient for desorbing carbon dioxide from activated carbons even at T<150°C, in agreement with literature indicating the CO_2 adsorption on activated carbon as a physisorption [8]. Coherently, the trend obtained for the CO_2 recovery by purge is complementary to that obtained for the CO_2 recovery by heating (Fig. 2c), namely monotonically decreasing with the desorption temperature, since less CO_2, still adsorbed on the activated carbon surface, remains to be desorbed.

Even though the N_2 purge makes it possible to increase the amount of CO_2 recovered, in addition to that recovered with the heating step, it also causes an undesirable dilution (i.e. N_2 purge ends up lowering the CO_2 purity). Since the dilution caused by the purge does not depend on the purge flow rate but only on the purge volume [9], the only way to limit it is to make the purge time very short. It is interesting to define a mean CO_2 concentration of the whole recovered stream (C_m), i.e. taking into account both the separate steps of heating and subsequent purge. Fig. 3a and b report the trend obtained for C_m and the corresponding CO_2 recovery as a function of the purge time (t_p). For each curve the initial state is the end of the heating step. The CO_2 purity decreases immediately with the introduction of the purge gas, whereas the CO_2 recovery is accordingly increased. The observed decreasing trend of C_m is obviously slower when the regeneration temperature is higher. Indeed, in this case, there is less CO_2 to desorb still remaining inside the bed, namely the majority of the whole CO_2 captured has already been desorbed during the heating step.

For each fixed value of CO_2 recovery it is possible, by elaborating the curves reported in Fig. 3, to obtain the value of CO_2 purity, thus obtaining a trend of C_m at the different desorption temperatures as a function of CO_2 recovery for the separate heating and purge strategy, as reported in Fig .4. The same curves obtained during the conventional isothermal purge [9] are reported for comparison in order to point out the optimized regeneration process. It is clear that for each desorption temperature the heating and purge strategy always makes it possible to enrich the stream of CO_2 recovered with respect to the isothermal purge strategy, the CO_2 recovery level being the same. However, at the lowest desorption temperatures (40 and 70°C) the difference between the two methods is not so remarkable since only a minor fraction of the total CO_2 captured is recovered due to heating, being the majority of the CO_2 still recovered by purge, thus making the two methods more or less equivalent. On the contrary, already at 100°C the difference starts becoming appreciable. Temperatures higher than 100°C are enough to obtain 100% vol. CO_2 purity with recovery levels higher than 50% and the maximum recovery still corresponding to a pure CO_2 stream increases with desorption temperatures. Obviously, even at the highest desorption temperatures, the trends of C_m

corresponding to the two different regeneration strategies tend to converge with increasing the CO_2 recovery level. Indeed, even though for temperatures higher than 100°C more than 70% of the CO_2 is recovered as a pure stream after the heating step, with increasing CO_2 recovery levels the purge time becomes large enough to cause a remarkable dilution effect.

3.2 Cyclic adsorption/desorption tests

Considering that a bland temperature of 130°C makes it possible to recover the 80% of the captured CO_2 with a 100% vol. purity, the possibility to realize a cyclic adsorption/desorption process has also been assessed. In particular, twenty TSA cyclic tests have been performed regenerating the sample by the sole heating (i.e. with no purging gas). The breakthrough curves have been elaborated to evaluate: (i) the amount of CO_2 adsorbed per unit mass of adsorbent, n_{ads}; (ii) the breakthrough time, t_b, which is the time it takes for CO_2 to be detected at the adsorption column outlet (5% of the inlet concentration); iii) the fraction of bed used at breakpoint (W), namely the ratio between the CO_2 adsorbed until the break point and that adsorbed until saturation. The results obtained are shown in Fig. 5.

The results obtained highlight the possibility to recover the captured CO_2 with a 100% vol. purity even in a cyclic process, thus eliminating the dilution side effect. This is made possible by completely removing the need of the purging gas to induce the sorbent regeneration. In particular, after the first adsorption step the CO_2 adsorption capacity of the activated carbon is reduced by about 20% with respect to that of the fresh sample, since a recovery level of 80% can be obtained using a desorption temperature of 130°C (i.e. the residual amount of CO_2 negatively influences the subsequent adsorption steps). Besides the CO_2 adsorption capacity, also t_b and W undergo a decrease with respect to the values obtained in the first adsorption step (namely using the fresh sample). Then, starting from the second adsorption phase, the activated carbon adsorption performances keep constant in all the following cycles, according to the stability of this activated carbon (as already shown in [9]).

4 Conclusions

Aiming to the enrichment of the recovered CO_2 stream by a conventional TSA process, the heating and purge regeneration strategy has been tested, consisting in desorbing part of the CO_2 by the sole thermal effect, thus eliminating the unavoidable dilution effect caused by purge, and the remainder reducing the CO_2 partial pressure. Heating is very efficient for desorbing carbon dioxide. The carbon dioxide recovery level increases with the regeneration temperature. 80% of the adsorbed carbon dioxide can be recovered at atmospheric pressure and at a bland desorption temperature of 130°C. In order to increase the operating capacity, the residual carbon dioxide can be eluted by a nitrogen purge. Obviously, the CO_2 purity decreases immediately with the introduction of the purge gas, whereas the CO_2 recovery is accordingly increased. It is worth noting that for each desorption temperature the heating and purge strategy always makes it possible to enrich the stream of CO_2 recovered with respect to a standard purge strategy, the CO_2 recovery level being the same. In particular starting from temperatures of 100°C, it is always possible to obtain 100% vol. CO_2 purity with recovery levels higher than 50%. Obviously, the maximum recovery still corresponding to a pure CO_2 stream increases with desorption temperatures.

Finally, twenty TSA cyclic tests have been performed regenerating the sample by the sole heating. The results obtained point out the possibility to recover CO_2 with a 100% vol. purity also in a cyclic process avoiding the necessity to use a purging gas during the CO_2 recovery.

5 Acknowledgements

This work was financially supported by the Accordo CNR-MSE ‘‘Utilizzo pulito dei combustibili fossili ai fini del risparmio energetico’’ 2011-2012 (Italy).

6 References

[1] C. Song, Global challenges and strategies for control, conversion and utilization of CO_2 for sustainable development involving energy, catalysis, adsorption and chemical processing, Catal. Today 115 (2006) 2–32.

[2] International Panel on Climate Control (IPCC), Carbon Dioxide Capture and Storage, Special Report International Panel on Climate Control, 2007.

[3] R.E. Hester, R.M. Harrision, Carbon capture sequestration and storage. Cambridge, UK: The Royal Society of Chemistry, 2010.

[4] J.D. Figueroa, T. Fout, S. Plasynski, H. McIlvried, R.D. Srivastava, Advances in CO_2 capture technology—The U.S. Department of Energy's Carbon Sequestration Program, Int. J. Greenh. Gas Con. 2 (2008) 9–20.

[5] R. Dawson, A.I. Cooper, D.J. Adams, Chemical functionalization strategies for carbon dioxide capture in microporous organic polymers, Polym. Int. 62 (2013) 345–352.

[6] Y. Yang, C. Sitprasert, T.E. Rufford, L .Ge, P. Shukla, S. Wang, V. Rudolph. Z. Zhu, An experimental and simulation study of binary adsorption in metal–organic frameworks, Sep. Purif. Technol. 146 (2015) 136–142.

[7] G.D. Pirngruber, F. Guillou, A. Gomez, M. Clausse, A theoretical analysis of the energy consumption of post-combustion CO_2 capture processes by temperature swing adsorption using solid sorbents, Int. J. Greenh. Gas Con. 14 (2013) 74–83.

[8] M.G. Plaza, S. García, F. Rubiera, J.J. Pis, C. Pevida, Post-combustion CO_2 capture with a commercial activated carbon: comparison of different regeneration strategies, Chem. Eng. J. 163 (2010) 41–47.

[9] P. Ammendola, F. Raganati, R. Chirone, Effect of operating conditions on the CO_2 recovery from a fine activated carbon by means of TSA in a fluidized bed assisted by acoustic fields, Fuel Process. Technol. 134 (2015) 494–501.

[10] F. Raganati, P. Ammendola, R. Chirone, Effect of acoustic field on CO_2 desorption in a fluidized bed of fine activated carbon, Particuology, 23 (2015) 8-15.

[11] D.M. D'Alessandro, B. Smit, J.R. Long, Carbon Dioxide Capture: Prospects for New Materials, Angew. Chem. Int. Ed. 49 (2010) 6058–6082.

[12] F.Y. Chang, K.J. Chao, H.H. Cheng, C.S. Tan, Adsorption of CO_2 onto amine-grafted mesoporous silicas, Sep. Purif. Technol. 70 (2009) 87–95.

[13] R.L Tseng, F.C. Wu, R.S. Juang, Adsorption of CO_2 at atmospheric pressure on activated carbons prepared from melamine-modified phenol–formaldehyde resins, Sep. Purif. Technol. 140 (2015) 53–60.

[14] R. Dawson, D.J. Adams, A.I. Cooper, Chemical tuning of CO_2 sorption in robust nanoporous organic polymers, Chem. Sci. 2 (2011) 1173–1177.

[15] J. Merel, M. Clausse, F. Meunier, Experimental investigation on CO_2 post-combustion capture by indirect thermal swing adsorption using 13X and 5A zeolites, Ind. Eng. Chem. Res. 47 (2008) 209–215.

[16] C. Chou, C. Chen, Carbon dioxide recovery by vacuum swing adsorption, Sep. Purif. Technol. 39 (2004) 51–65.

[17] C.A. Grande, R.P.L. Ribeiro, E.L.G. Oliveira, A. Rodrigues, Electric swing adsorption as emerging CO_2 capture technique, Energy Procedia 1 (2009) 1219–1225.

[18] N. Tlili, G. Grévillot, C. Vallières, Carbon dioxide capture and recovery by means of TSA and/or VSA. Int. J. Greenh. Gas Con. 3 (2009) 519–527.

[19] W.C. Yang, J. Hoffman, Exploratory Design Study on Reactor Configurations for Carbon Dioxide Capture from Conventional Power Plants Employing Regenerable Solid Sorbents, Ind. Eng. Chem. Res. 48 (2009) 341–351.

[20] S. Sjostrom, H. Krutka, T. Starns, T. Campbell, Pilot test results of post-combustion CO_2 capture using solid sorbents, Energy Procedia 4 (2011) 1584–1592.

[21] X. Wang, R.F. Rahman, M.J. Rhodes, Nanoparticle fluidization and Geldart's classification, Chem. Eng. Sci. 62 (2007) 3455–3461.

[22] P. Ammendola, R. Chirone, Aeration and mixing behaviours of nano-sized powders under sound vibration. Powder Technol. 201 (2010) 49–56.

[23] F. Raganati, P. Ammendola, R. Chirone, Role of Acoustic Fields in Promoting the Gas-Solid Contact in a Fluidized Bed of Fine Particles, KONA Powder Part. J. 32 (2015) 23–40.

[24] P. Ammendola, R. Chirone, F. Raganati, Effect of mixture composition, nanoparticle density and sound intensity on mixing quality of nanopowders, Chem. Eng. Process. Process Intens. 50 (2011) 885–891.

[25] P. Ammendola, R. Chirone, F. Raganati, Fluidization of binary mixtures of nanoparticles under the effect of acoustic fields, Adv. Powder Technol. 22 (2011) 174–183.

[26] M. Kashyap, D. Gidaspow, M. Driscoll, Effect of electric field on the hydrodynamics of fluidized nanoparticles, Powder Technol. 183 (2008) 441–53

[27] P. Zang, J. Yang, Behaviour of mixture of nano-particles in magnetically assisted fluidized bed, Chem. Eng. Process. 47 (2008) 101–8.

[28] S. Kaliyaperumal, S. Barghi, L. Briens, S. Rohani, J. Zhu, Fluidization of nano and sub-micron powders using mechanical vibration, Particuology 9 (2011) 279–287.

[29] F. Raganati, P. Ammendola, R. Chirone, CO_2 adsorption on fine activated carbon in a sound assisted fluidized bed: Effect of sound intensity and frequency, CO_2 partial pressure and fluidization velocity, Appl. Energ. 113 (2014) 1269–1282.

[30] J.M. Valverde, F. Raganati, M.A.S. Quintanilla, J.M. Ebri, P. Ammendola, R. Chirone, Enhancement of CO_2 capture at Ca-looping conditions by high-intensity acoustic fields, Appl. Energ. 111 (2013) 538–549.

[31] F. Raganati, P. Ammendola, R. Chirone, CO_2 capture performances of fine solid sorbents in a sound-assisted fluidized bed, Powder Technol. 268 (2014) 347–356.

[32] F. Raganati, V. Gargiulo, P. Ammendola, M. Alfe, R. Chirone, CO_2 capture performance of HKUST-1 in a sound assisted fluidized bed, Chemi. Eng. J. 239 (2014) 75–86.

[33] M. Alfe, P. Ammendola, V Gargiulo, F. Raganati, R. Chirone, Magnetite loaded carbon fine particles as low-cost CO_2 adsorbent in a sound assisted fluidized bed. P. Combust. Inst. 35 (2015) 2801–2809.

Figure captions

Fig. 1 Experimental apparatus: (1) N_2 cylinder; (2) CO_2 cylinder (3) N_2 flow meter; (4) CO_2 flow meter; (5) controller; (6) 40 mm ID fluidization column; (7) filter; (8) microphone; (9) sound guide; (10) wind-box; (11) pressure transducer; (12) CO_2 analyzer; (13) loudspeaker; (14) pump; (15) stack; (16) thermocouple; (17) temperature controller; (18) heating jacket; (19) two-way valve; (20) gas sampling probe; (21) volumetric flow meter.

Fig. 2 a) Total outlet flow rate during desorption by heating; b) CO_2 outlet concentration profiles during the purge step; c) CO_2 recovery during heating and purge as function of desorption temperature. Purge step: N_2 purge flow rate=67.8 Nl h^{-1}; SPL=140 dB; Sound frequency=80 Hz. Adsorption step: SPL=140 dB; Sound frequency=80 Hz; inlet flow rate=67.8 Nl h^{-1}; C_0=10% vol.

Fig. 3 CO_2 mean concentration (a) and recovery (b) as function of purge time at different desorption temperatures. Purge step: N_2 purge flow rate=67.8 Nl h^{-1}; SPL=140 dB; Sound frequency=80 Hz. Adsorption step: SPL=140 dB; Sound frequency=80 Hz; inlet flow rate=67.8Nl h^{-1}; C_0=10% vol.

Fig. 4 CO_2 mean concentration as function of recovery obtained with the isothermal purge [9] and heating and purge strategies at different desorption temperatures. Purge step: N_2 purge flow rate=67.8Nl h^{-1}; SPL=140 dB; Sound frequency=80 Hz. Adsorption step: SPL=140 dB; Sound frequency=80 Hz; inlet flow rate=67.8Nl h^{-1}; C_0=10% vol.

Fig. 5 CO_2 adsorption performances vs the number of cycles. A Cycle is made of : Adsorption step, SPL=140 dB; Sound frequency=80 Hz; inlet flow rate=67.8 Nl h^{-1}; C_0=10% vol. and desorption step: only heating, temperature = 130°C.

Table captions

Table 1 CO_2 recovery during the heating and purge steps.

Tables

Table 1

T_{des}, °C	Recovery by Heating, %	Recovery by Purge, %	Total, %
40	17.73	82.07	99.8
70	48.02	51.18	99.2
100	66.94	32.46	99.4
130	79.53	19.77	99.3
150	81.73	17.67	99.4

Figures

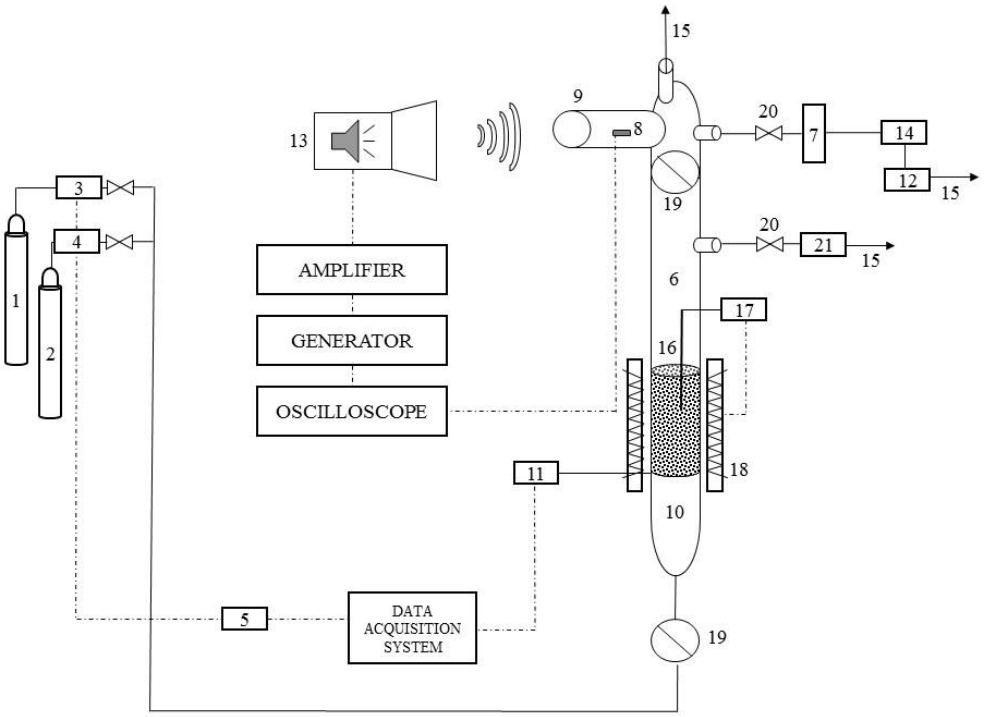

Fig. 1

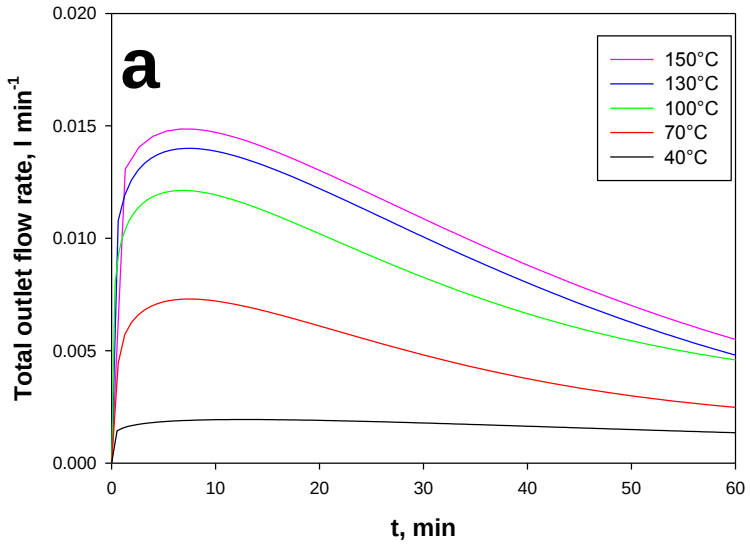
a
Total outlet flow rate, l min-1
0.020
0.015
0.010
0.005
0.000
0
10
20
30
40
50
60
t, min
150°C
130°C
100°C
70°C
40°C

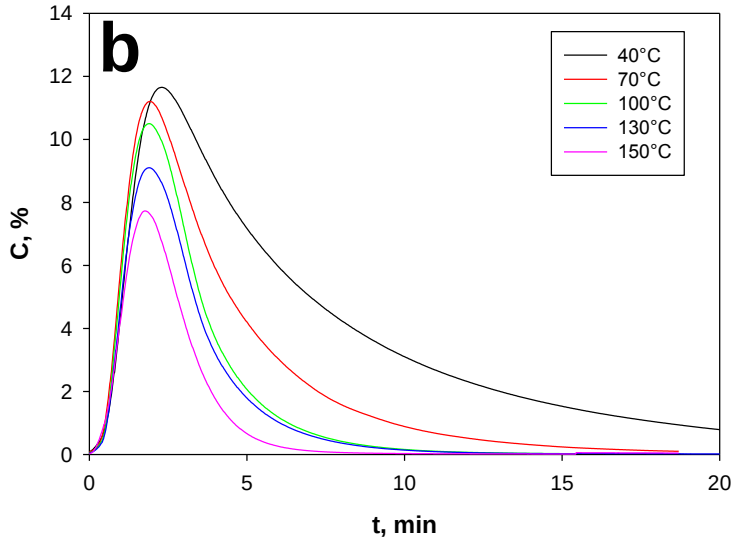
b
C, %
14
12
10
8
6
4
2
0
0
5
10
15
20
t, min
40°C
70°C
100°C
130°C
150°C

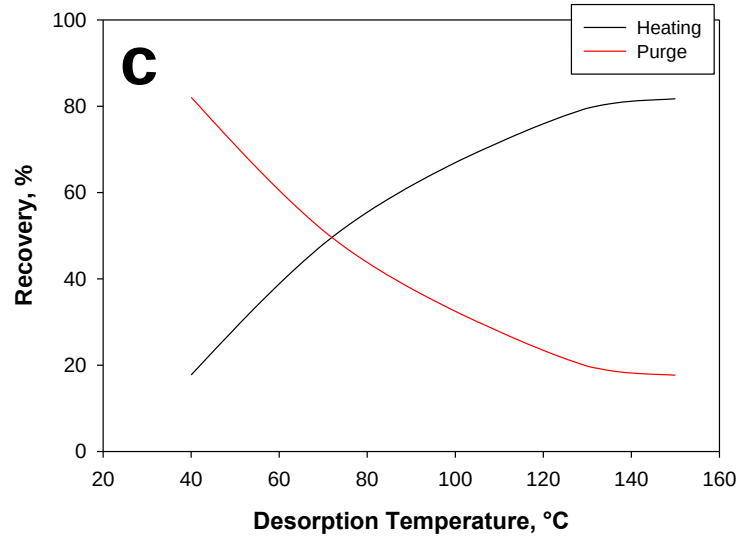
c
Recovery, %
100
80
60
40
20
0
20
40
60
80
100
120
140
160
Desorption Temperature, °C
Heating
Purge

Fig. 2

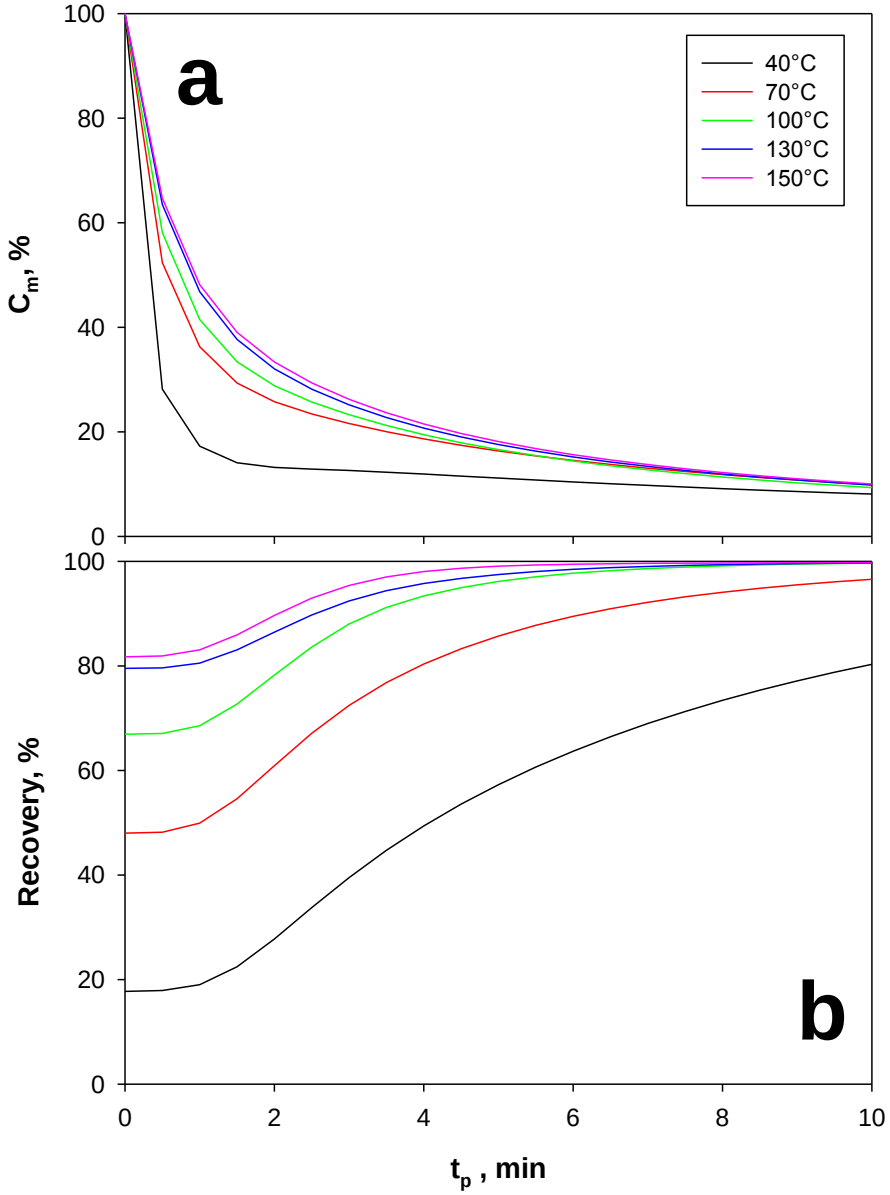
a
b
40°C
70°C
100°C
130°C
150°C
C_m, %
Recovery, %
t_p , min
0
20
40
60
80
100
0
2
4
6
8
10

Fig. 3

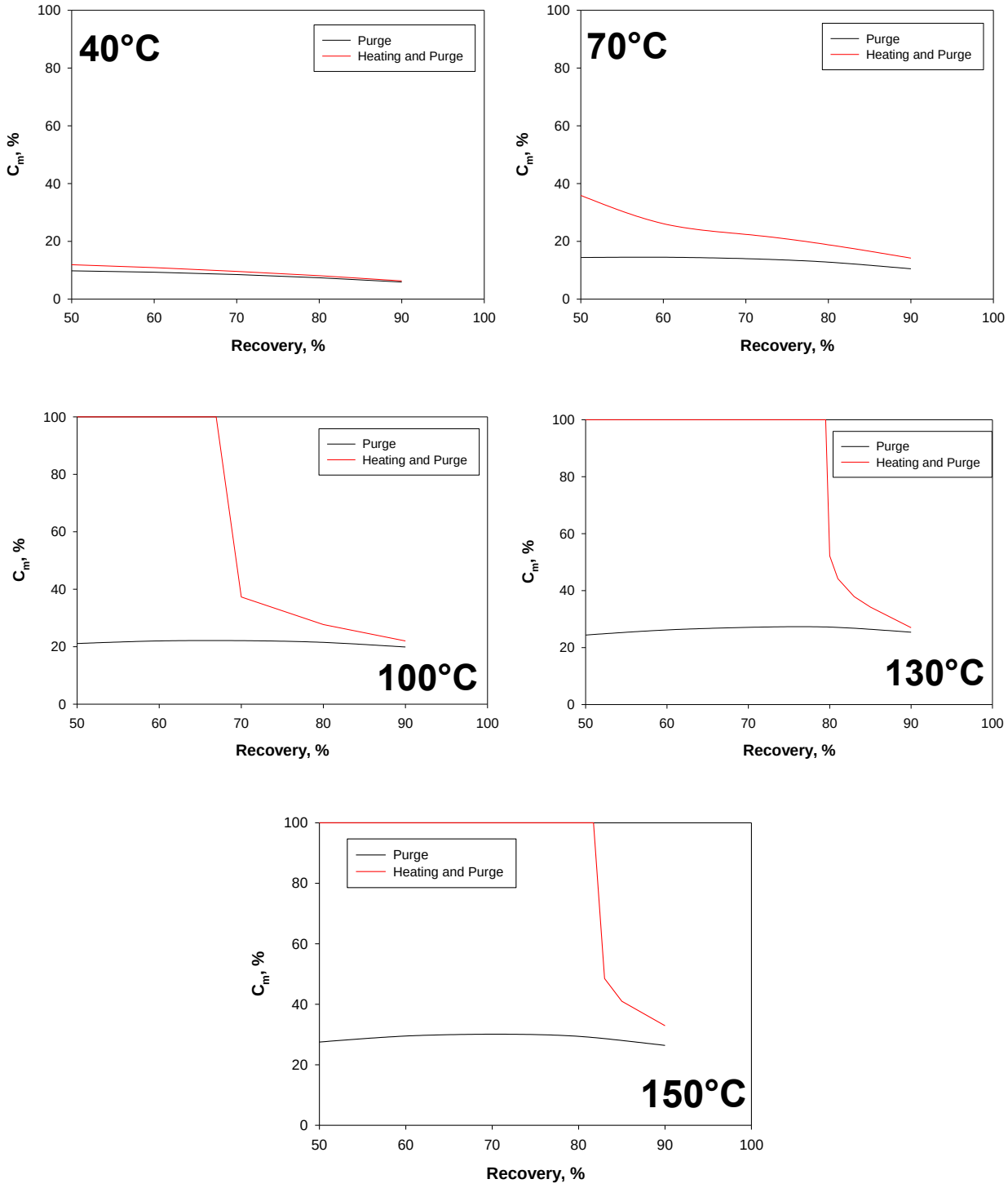
40°C
70°C
100°C
130°C
150°C
Purge
Heating and Purge
C_m, %
Recovery, %
0
20
40
60
80
100
50
60
70
80
90
100

Fig. 4

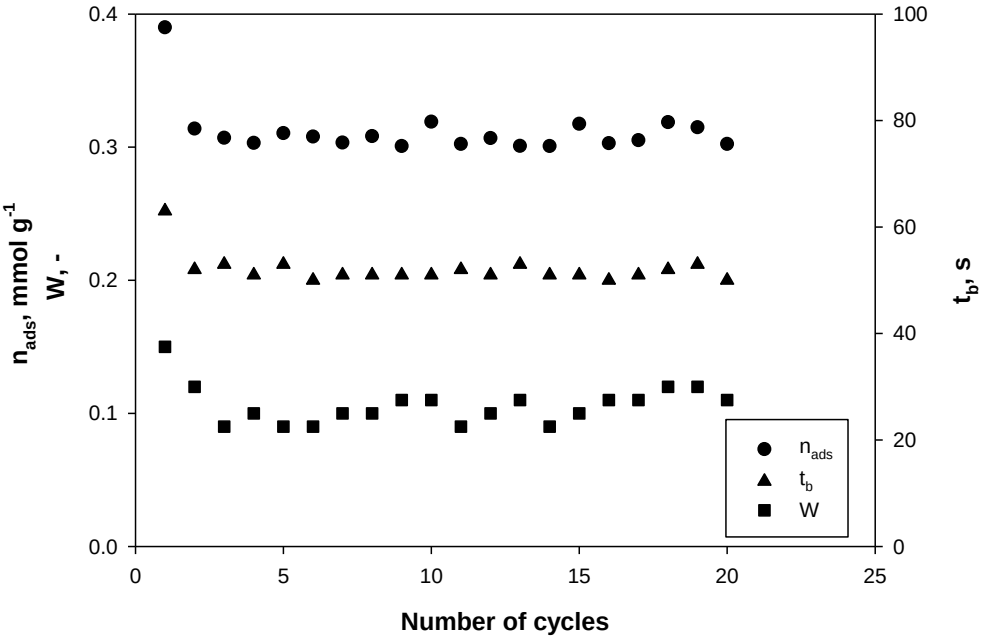
0.4
0.3
0.2
0.1
0.0
100
80
60
40
20
0
0
5
10
15
20
25
Number of cycles
n_{ads}, mmol g^{-1}
W, -
t_b, s
n_{ads}
t_b
W

Fig. 5

***List of Potential Reviewers**

Prof. Brunello Formisani
Dipartimento di Ingegneria per l'Ambiente e il Territorio e Ingegneria Chimica
Università della Calabria
Via Pietro Bucci - 87036 - Arcavacata di Rende (CS) - Italy
e-mail: bruno.formisani@unical.it

Dr. Paola Lettieri
Department of Chemical Engineering
University College London
Torrington Place
London WC1E 7JE, UK
Tel: +44 (0) 20 7679 7867
Fax: +44 (0) 20 7383 2348
E-mail: p.lettieri@ucl.ac.uk

Prof. Jamal Chaouki
Department of Chemical Engineering, Ecole Polytechnique de Montreal
P.O. Box 6079, Station Centre-Ville, Montreal, Quebec, Canada, H3C 3A7.
e-mail: jamal.chaouki@polymtl.ca

Dr. Ray Cocco
Particulate Solid Research, Inc. (PSRI)
4201 West 36th Street, Suite 200
Chicago, IL, USA 60632
e-mail: ray.cocco@psrichicago.com